

# Weak Lensing of Galaxy Clusters in MOND

Ryuichi Takahashi<sup>1</sup> and Takeshi Chiba<sup>2</sup>

<sup>1</sup> Division of Theoretical Astronomy, National Astronomical Observatory of Japan, Mitaka, Tokyo 181-8588, Japan

<sup>2</sup> Department of Physics, College of Humanities and Sciences, Nihon University, Tokyo 156-8550, Japan

## ABSTRACT

We study weak gravitational lensing of galaxy clusters in terms of the relativistic MOND (MOdified Newtonian Dynamics) theory proposed by Bekenstein (2004). We calculate shears and magnifications of background galaxies for three clusters (A1689, CL0024+1654, CL1358+6245) and 42 SDSS (Sloan Digital Sky Survey) clusters and compare them with observational data. The mass profile is modeled as a sum of X-ray gas, galaxies and dark halo. For the shear as a function of the angle from the lens center, MOND predicts a shallower slope than the data irrespective of the critical acceleration parameter  $g_0$ . The dark halo is necessary to explain the data for any  $g_0$ . If the dark halo is composed of massive neutrinos, its mass should be heavier than 2 – 3 eV. However, it is still difficult to explain a small core (100 – 300 kpc) determined by the lensing data in the neutrino halo model.

*Subject headings:* cosmology: theory – galaxies: clusters: individual (A1689, CL0024+1654, CL1358+6245) – gravitation – gravitational lensing

## 1. Introduction

MOND (MOdified Newtonian Dynamics) is a theoretical alternative to Newtonian dynamics, proposed by Milgrom (1983). The theory itself strengthens gravitational force at large distances (or small accelerations) to explain galactic dynamics without dark matter. The equation of motion is changed if the acceleration is lower than the critical value  $g_0 \simeq 1 \times 10^{-8} \text{ cm/s}^2 \approx H_0$ . It is well known that this theory can explain galactic rotation curves with only one free parameter: the mass-to-light ratio (see review Sanders & McGaugh 2002). There are two motivations to study such an alternative theory: (i) General Relativity (GR) has not been tested accurately at much larger scale than 1 AU (ii) dark matter particles have not been directly detected and their nature still eludes us. Under these circumstances, several authors have recently studied alternative theories to GR (e.g. Aguirre 2003).

Bekenstein (2004) recently proposed a relativistic covariant formula of MOND (called TeVeS) by introducing several new fields and param-

eters. Following this, several authors began discussing relativistic phenomena such as parameterised Post-Newtonian formalism in the solar system (Bekenstein 2004), gravitational lensing (e.g. Zhao et al. 2006), cosmic microwave background and large scale structure of the Universe (Slosar et al. 2005; Skordis 2005; Skordis et al. 2006). In this paper, we discuss weak gravitational lensing of galaxy clusters.

This weak lensing provides an important observational method with which to test MOND. This is because the weak lensing probes the lens potential outside of the Einstein radius,  $r_E \sim (MD)^{1/2} \simeq 150 \text{ kpc} (M/10^{14} M_\odot)^{1/2} (D/H_0^{-1})^{1/2}$ , where  $M$  is the lens mass and  $D$  is the distance to the source. The gravitational law changes outside the MOND radius,  $r_M = (M/g_0)^{1/2}$ , where the acceleration is less than  $g_0$ . Since  $g_0 \approx H_0 \approx 1/D$ , the Einstein radius  $r_E$  is comparable to the MOND radius  $r_M$ . Hence, we can test the MOND-gravity regime by the weak lensing.

Weak lensing is superior to X-rays as a means of probing the outer region of clusters. The lensing

signal (strength of the shear) is proportional to the cluster density  $\rho$ . On the other hand, the X-ray luminosity is proportional to  $\rho^2$  and hence X-rays can probe the inner regions of clusters. Hence, the outer region of the clusters can be probed with weak lensing.

The gravitational lensing in MOND has been studied by many authors. Before Bekenstein proposed the relativistic formula, some assumptions were made<sup>1</sup> to calculate the lensing quantities (Qin et al. 1995; Mortlock & Turner 2001a; 2001b; White & Kochanek 2001; Gavazzi 2002). Just after Bekenstein's proposal, Chiu et al. (2006) and Zhao et al. (2006) first studied the lensing in detail and tested MOND with strong lensing data of galaxies. Zhao and his collaborators studied the gravitational lens statistics (Chen & Zhao 2006) and investigated a non-spherical symmetric lens (Angus et al. 2006). Recently, Clowe et al. (2006) indicated that a merging cluster 1E 0657-558 cannot be explained by MOND because the weak lensing mass peak is  $8\sigma$  spatial offset from the baryonic peak (= mass peak of X-ray gas). However, Angus et al. (2006) noted that MOND can explain the data if the neutrino halo is included.

In this paper, we study three clusters (A1689, CL0024+1654, CL1358+6245) and 42 SDSS (Sloan Digital Sky Survey) clusters. We calculate shears and magnifications for these clusters and compare them with the observational data. We perform a  $\chi^2$  fit of the data to give a constraint on the dark halo profile and the neutrino mass. Throughout this paper, we use the units of  $c = G = 1$ .

## 2. Basics

We briefly review the basics of gravitational lensing based on the relativistic MOND theory for a spherically symmetric lens model. Detailed discussions are given in Bekenstein (2004) and Zhao et al. (2006).

When a light ray passes through a lens with the impact parameter  $b$ , the deflection angle is

$$\alpha(b) = 2b \int_{-\infty}^{\infty} dl \frac{g(r)}{r}, \quad (1)$$

<sup>1</sup>For example, Qin et al. (1995) assumed that the bending angle is 2 times larger than that for massive particles in the limit of  $m \rightarrow 0$ . This is an analogy to GR.

where  $l$  is the distance along the light path and  $r$  is the distance from the lens center,  $r = \sqrt{l^2 + b^2}$  (see Fig.1).

The gravitational force due to the lens is

$$\tilde{\mu}(g/g_0)g(r) = g_N(r) = \frac{M(< r)}{r^2}, \quad (2)$$

where  $g_N$  is the usual Newtonian acceleration and  $M(< r)$  is the lens mass enclosed inside a radius  $r$ . We use a standard interpolation function  $\tilde{\mu}(x) = x/\sqrt{1+x^2}$  with  $g_0 = 1 \times 10^{-8} \text{ cm s}^{-2}$ . Then,  $\tilde{\mu}(x) = 1$  (i.e.  $g = g_N$ ) for  $g \gg g_0$ , while  $\tilde{\mu}(x) = x$  (i.e.  $g = \sqrt{g_N g_0}$ ) for  $g \ll g_0$ .

The lens equation is

$$\theta_s = \theta - \frac{D_{LS}}{D_S} \alpha(\theta). \quad (3)$$

Here,  $\theta_s$  and  $\theta (= b/D_L)$  are the angular positions of the source and the image, and  $D_L$ ,  $D_S$  and  $D_{LS}$  are the angular diameter distances between the observer, the lens and the source.<sup>2</sup> The shear  $\gamma$  and the convergence  $\kappa$  are given by,

$$\gamma = \frac{1}{2} \left[ \frac{\theta_s}{\theta} - \frac{d\theta_s}{d\theta} \right]; \quad 1 - \kappa = \frac{1}{2} \left[ \frac{\theta_s}{\theta} + \frac{d\theta_s}{d\theta} \right] \quad (4)$$

We note that if the mass increases as  $M \propto r^p$  with  $p \geq 0$ , the shear and the convergence decrease as

$$\gamma \propto \kappa \propto \begin{cases} \theta^{p-2} & \text{for } g \gg g_0, \\ \theta^{p/2-1} & \text{for } g \ll g_0, \end{cases} \quad (5)$$

from Eqs.(1)-(4). The slopes of  $\gamma$  and  $\kappa$  for  $g \gg g_0$  are steeper than that for  $g \ll g_0$ . This is because

<sup>2</sup>We use the distance in the usual FRW (Friedmann-Robertson-Walker) model with  $\Omega_M = 1 - \Omega_\Lambda = 0.3$  and  $H_0 = 70 \text{ km/s/Mpc}$ . The distance in MOND is almost the same as that in the FRW model (Bekenstein 2004).

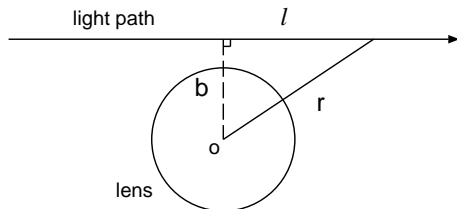


Fig. 1.— A schematic picture of the light ray passing through the lens.

the gravitational force is proportional to  $g_N^{1/2}$  for  $g \ll g_0$ , and hence the force decreases more slowly at larger distances. Comparing the slope in Eq.(5) with the observational data, we can test MOND.

We also give the magnification of the lensed image

$$\mu = \left| \frac{d\theta_s}{d\theta} \frac{\theta_s}{\theta} \right|^{-1}. \quad (6)$$

### 3. Analysis with Cluster Data

We calculate the shear  $\gamma$ , the convergence  $\kappa$  and the magnification  $\mu$  based on the MOND theory for the three clusters, A1689, CL0024+1654, CL1358+6245, and 42 SDSS clusters. The mass profiles of these clusters have been measured by gravitational lensing for a wider range of angular diameters, and hence these clusters are an appropriate system to investigate the angle-dependence of the shear and the convergence. In this section, we assume the source redshift is  $z_S = 1$ .

#### 3.1. A1689

The mass profile of the cluster A1689<sup>3</sup> is shown in Fig.2(a). The hot gas mass profile was directly determined from X-ray observational data (Andersson & Madejski 2004). The galaxy mass profile was given from the surface brightness profile, assuming the constant mass-to-light ratio  $8M_\odot/L_\odot$  (B-band) (Zekser et al. 2006). The total baryonic mass (gas + galaxies) is shown in the solid line. We also show the dark halo profile which will be needed to match the observational data (we will discuss this later).

Fig.2(b) shows the Newtonian gravitational acceleration  $g_N$  normalized to  $g_0$ . As shown in this panel, the transition radius corresponding to  $g_N = g_0$  (denoted by a horizontal dotted line) is 100 kpc for the gas + galaxies and is at 1000 kpc if the dark halo is added.

Panel (c) shows the reduced shear data  $\gamma/(1-\kappa)$  from Broadhurst et al. (2005). The solid line is the MOND theoretical prediction. We note that for  $\theta < 10'$  the solid line is clearly smaller than the data. This indicates that the gravitational force is too weak to explain the data. In order to solve this discrepancy, we need a very high mass-to-right ra-

<sup>3</sup>Its redshift is  $z = 0.183$  and  $1'$  corresponds to 184kpc.

tio  $\sim 200M_\odot/L_\odot$ <sup>4</sup>. On the dotted line, for the critical acceleration  $g_0$  we use 40 times larger than the usual value ( $= 1 \times 10^{-8} \text{cm s}^{-2}$ ). In this case, for the central region ( $\theta < 4'$ ) the theory can explain the data, but for a larger radius it cannot. This is because  $g < g_0$  for the angle of  $\theta > 0.5'$  ( $\leftrightarrow r > 100 \text{kpc}$ ) from panel (b) and hence the slope of shear is shallow from Eq.(5). The slope is shallower than  $\gamma \propto \theta^{-1}$  for  $g < g_0$  (since  $p \geq 0$  in Eq.(5)) and the data in panel (c) clearly shows a steeper profile than this. Hence MOND cannot explain the data for any mass model and any acceleration parameter  $g_0$  in the low acceleration region  $g < g_0$ .

The lensing magnification  $\mu$  expands the area of sky and amplifies the flux of background galaxies. The number counts of galaxies  $N$  behind the cluster are changed by this magnification effect (Broadhurst et al. 1995) :  $N/N_0 = \mu^{2.5s-1}$  where  $N_0$  is the unlensed counts and  $s$  is the slope of the background galaxy luminosity function. Panel (d) shows the magnification bias  $\mu^{2.5s-1}$  with  $s = 0.22$ . For the solid (dotted) line, the magnification bias is too strong (weak) to match the data.

Previously, Aguirre, Schaye & Quataert (2001), Sanders (2003), and Pointecouteau & Silk (2005) reached the same conclusion as ours by studying temperature profiles of clusters. They indicated that the temperature data near the core is higher than the MOND prediction. Sanders (2003) noted that if the dark matter core were added, this discrepancy could be resolved. Following the previous studies, we include the dark halo to explain the observational data. We take the Hernquist profile,

$$M(< r) = M_0 r^2 / (r + r_0)^2, \quad (7)$$

as the dark halo profile. We perform a  $\chi^2$  fit of the data in order to determine the parameters  $M_0$  and  $r_0$ . The  $\chi^2$  is given by  $\chi^2 = \sum_i (x_i - x_i^{data})^2 / \sigma_i^2$  where  $x_i$  is the reduced shear  $\gamma/(1-\kappa)$  at the  $i$ -th angle,  $x_i^{data}$  is the data and  $\sigma_i$  is the standard deviation. Here we use only the shear data, since the magnification data contain a large error. The best fitted model is  $M_0 = (6.2 \pm 1.2) \times 10^{14} M_\odot$  and  $r_0 = 125 \pm 52$  kpc (see Table 1). The minimized  $\chi^2$ -value per degree of freedom (dof) is  $\chi_{min}^2/\text{dof}$

<sup>4</sup>The shear and the convergence are proportional to the mass-to-light ratio  $M/L$  for  $g \gg g_0$ , while  $(M/L)^{1/2}$  for  $g \ll g_0$ .

$= 3.0/8$ . The results are insensitive to the mass-to-light ratio. As shown in panels (b) and (c), this model (dashed line) fits the data well. The dashed line in panel (c) is steeper than the solid and dotted lines, since  $\theta < 5'$  ( $\leftrightarrow r < 1000$ kpc) is the high acceleration region  $g > g_0$  from panel (b) and hence the slope is steeper, as can be seen in Eq.(5).

### 3.2. CL0024+1654

The redshift is  $z = 0.395$  and  $1'$  corresponds to 320 kpc. Fig.3(a) shows the mass distribution of the gas (Zhang et al. 2005), the galaxies with a mass-to-right ratio  $8M_\odot/L_\odot$  (K-band) (Kneib et al. 2003), and the dark halo. For the larger radius  $> 3$  Mpc the baryonic mass exceeds the dark halo mass. This is because we extrapolate the gas profile (fitted by isothermal  $\beta$  model for  $r \lesssim 1$  Mpc) to the larger radius. Panels (c) and (d) show the reduced shear (Kneib et al. 2003) and the magnification bias (Dye et al. 2002). Similar to the previous case of A1689, for  $\theta < 10'$  the solid line is smaller than the data, and we need the  $\sim 30M_\odot/L_\odot$  to solve this discrepancy. On the dotted line, the quantity  $g_0$  is 5 times larger than the usual value ( $= 1 \times 10^{-8}$ cm/s $^2$ ). The best fitted halo model is  $M_0 = (3.5 \pm 1.0) \times 10^{14} M_\odot$  and  $r_0 = 309 \pm 93$  kpc in Eq.(7) with  $\chi^2_{min}/dof = 9.9/8$ . Same as the previous case of A1689, the dark halo is needed to fit the data.

### 3.3. CL1358+6245

The redshift is  $z = 0.33$  and  $1'$  corresponds to 280 kpc. Fig.3(a) shows the mass distribution of the gas (Arabadjis et al. 2002), the galaxies with a mass-to-right ratio  $8M_\odot/L_\odot$  (V-band) (Hoekstra et al. 1998), and the dark halo. Panels (c) and (d) show the reduced shear and the magnification bias (Hoekstra et al. 1998). In panel (c), we need the  $\sim 30M_\odot/L_\odot$  to fit the data if we assume only baryonic components. On the dotted line, the quantity  $g_0$  is 6 times larger than the usual value. The best fitted model is  $M_0 = (8.1 \pm 3.6) \times 10^{13} M_\odot$  and with  $r_0 = 134 \pm 68$  kpc with  $\chi^2_{min}/dof = 4.5/7$ . Although the discrepancy between the MOND prediction and the data is not so large in comparison with the previous cases, the dark halo model is the better.

### 3.4. SDSS clusters

Sheldon et al. (2001) studied weak lensing of 42 clusters in SDSS data. They provided the mean shear of 42 clusters up to the radius of 2700 kpc as shown in Fig.5. The vertical axis is  $\Sigma_{cr}\gamma$ , where  $\Sigma_{cr} = 1/(4\pi)D_S/(D_L D_{LS})$  is the critical surface density, and the horizontal axis is the projected radius<sup>5</sup>. The data is well fitted by a power law with index  $-0.9 \pm 0.3$  (Sheldon et al. 2001). On the solid and dotted lines, we consider only the gas component, given by the isothermal beta model:

$$\rho(r) = \rho_0 \left[ 1 + \left( \frac{r}{r_c} \right)^2 \right]^{-3\beta/2}, \quad (8)$$

with  $\beta = 0.6$ ,  $r_c = 100$  kpc,  $\rho_0/\rho_{cr} = 8000$  (solid line) and 800 (dotted line), here  $\rho_{cr}$  is the critical density at the present. As shown in the figure, the fit is poor. This is because the slope of the shear is  $-3\beta/2 + 1/2 = -0.4$  for  $g < g_0$  and it is flatter than the data. The dashed line is the dark halo model (Hernquist profile). The best fitted model is  $M_0 = (3.82 \pm 1.14) \times 10^{13} M_\odot$  and  $r_0 = 123 \pm 61$  kpc with  $\chi^2_{min}/dof = 10.1/7$ . The dashed line fits the data well.

## 4. Limit on Neutrino Mass

In previous studies, several authors assumed a massive neutrino with a mass of  $\sim 2$  eV as the dark matter to explain the observational data (e.g. Sanders 2003; Skordis et al. 2006). In this section, we put a constraint on its mass from the weak lensing.

The neutrino oscillation experiments provide the mass differences between different species :  $\Delta m_\nu^2 \lesssim 10^{-3}$ eV $^2$ . Here we consider massive neutrinos whose masses are much heavier than  $\Delta m_\nu$  and assume they are degenerate: they have (almost) the same mass, independent of species. Using the maximum phase space density  $h^{-3}$ , the maximum density of the neutrino dark halo is given by  $\rho_{\nu max} = 4.8 \times 10^{-27} \text{g cm}^{-3} (m_\nu/2\text{eV})^4 (T/\text{keV})^{3/2}$  (Tremaine & Gunn 1979; Sanders 2003). The core density of the Hernquist profile is  $\rho_c = 3M(< r_0)/(4\pi r^3)$  from Eq.(7). Since  $\rho_c < \rho_{\nu max}$ , we obtain the

<sup>5</sup>The quantity  $\Sigma_{cr}\gamma$  is related to the surface density of the lens in GR :  $\Sigma_{cr}\gamma = \bar{\Sigma}(\leq R) - \Sigma(R)$ .

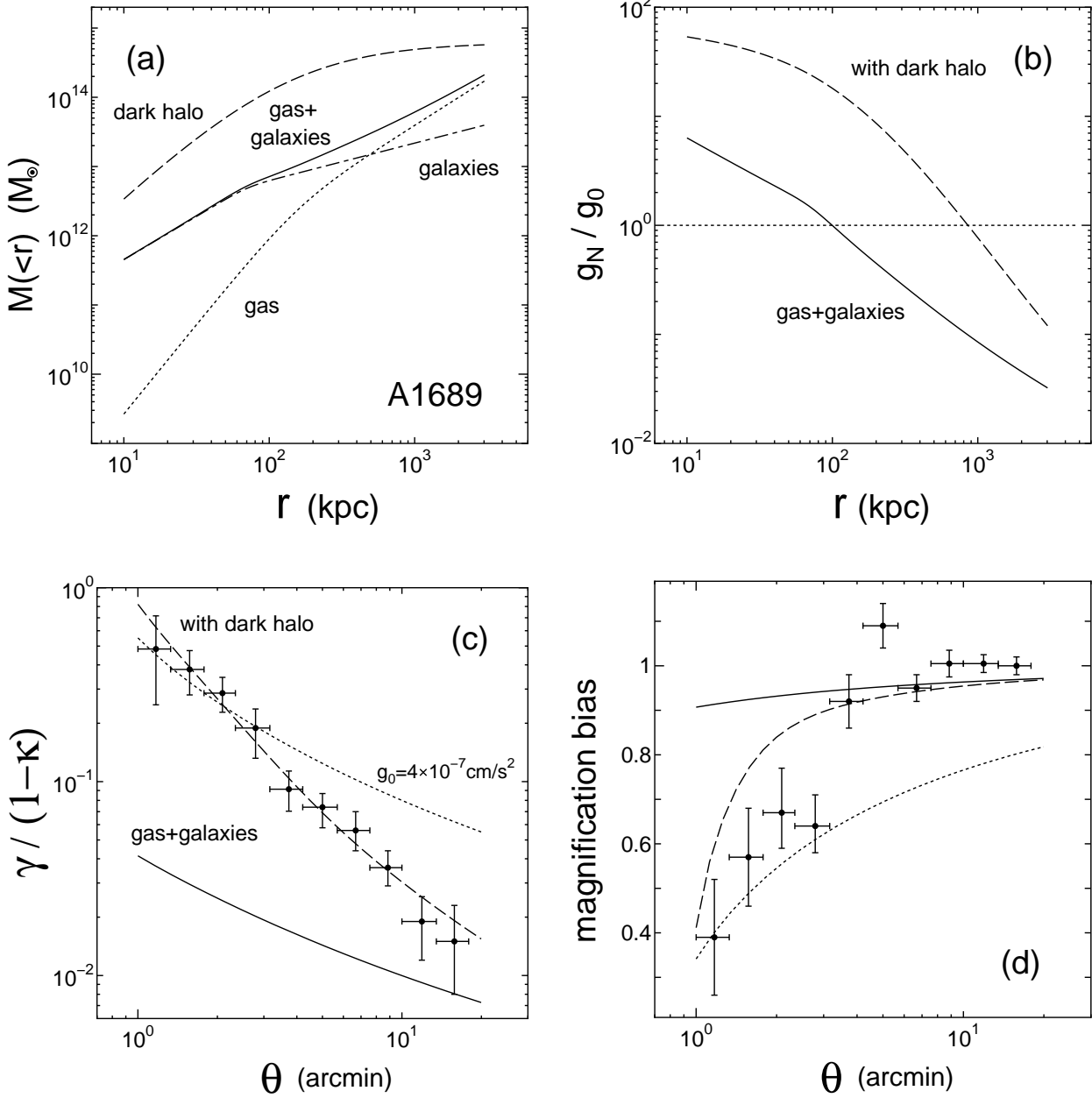


Fig. 2.— Results for the cluster A1689. The top left panel (a): The mass profiles of the gas (dotted line), the galaxies (dot-dashed line), the gas + galaxies (solid line), and the dark halo (dashed line). The quantity  $M(< r)$  is the mass enclosed within the radius  $r$ . The top right panel (b): The Newtonian gravitational acceleration  $g_N$  normalised to  $g_0$  for only baryonic components (gas + galaxies) (solid line) and all components (dark halo is added) (dashed line). The left bottom panel (c): The reduced shear  $\gamma/(1 - \kappa)$  as a function of an angle from the cluster center. The data is from Broadhurst et al. (2005). The solid line is the MOND prediction. On the dotted line we use the value of  $g_0$ , 40 times larger than the usual one ( $= 1 \times 10^{-8} \text{ cm/s}^2$ ). On the dashed line, the dark halo is added. The right bottom panel (d): The magnification bias,  $N/N_0 = \mu^{2.5s-1}$  with  $s = 0.22$ . From panels (c) and (d), the MOND cannot explain the data unless the dark halo is added, because the gravitational force is too weak near the core.

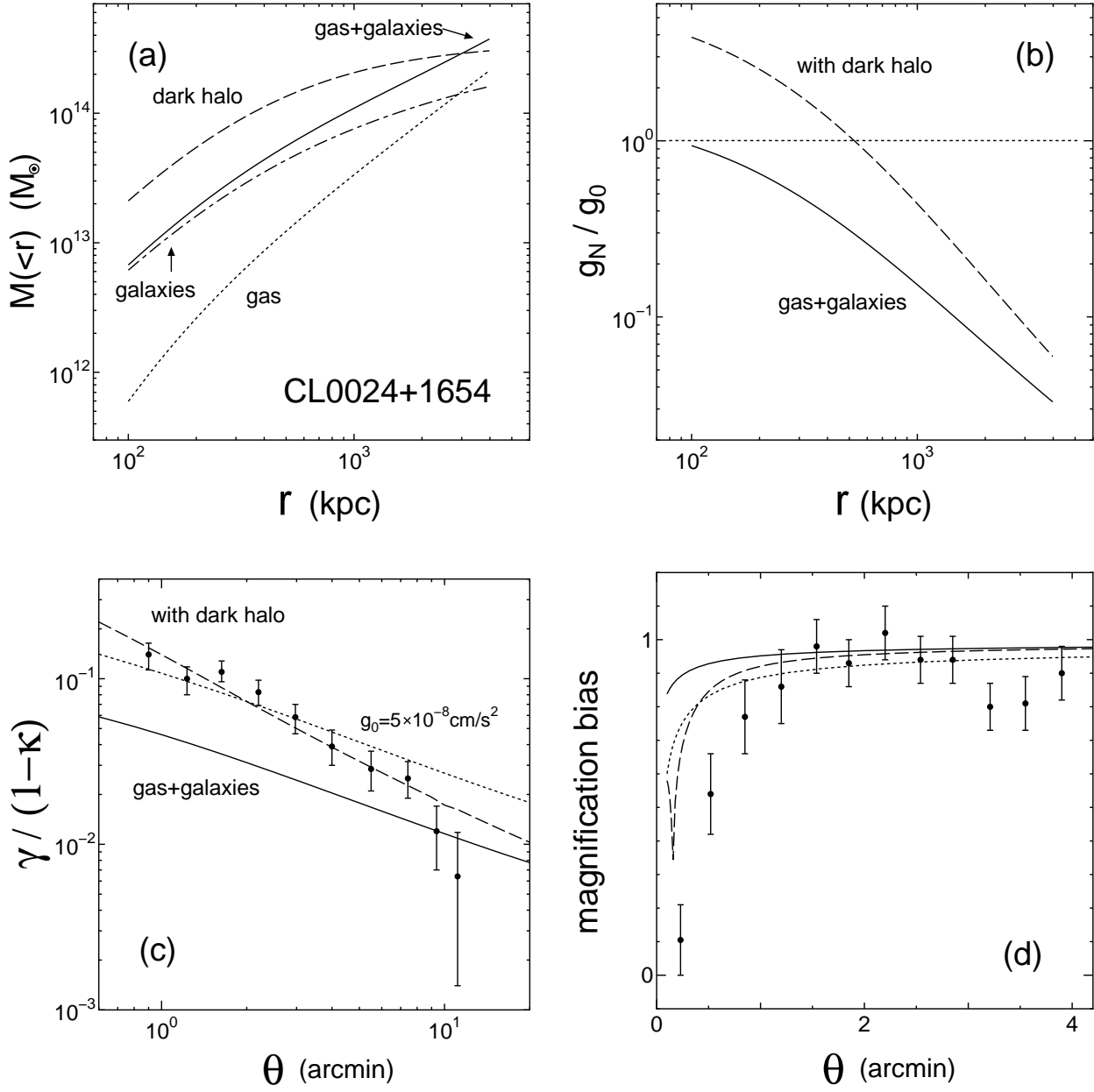


Fig. 3.— Same as Fig.2, but for the cluster CL0024+1654.

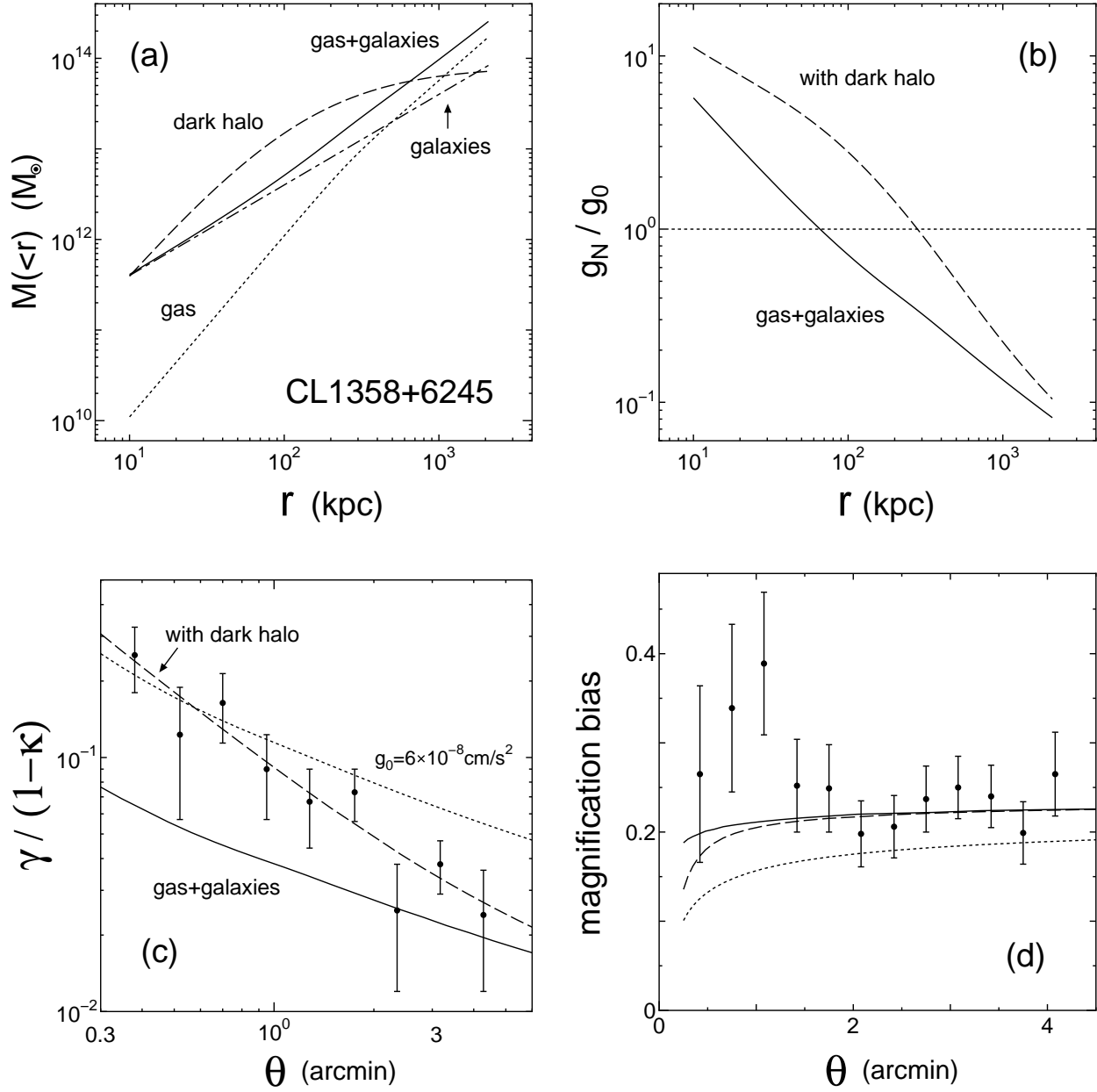


Fig. 4.— Same as Fig.2, but for the cluster CL1358+6245.

minimum neutrino mass,

$$m_\nu > 6.1 \text{eV} \left( \frac{M_0}{10^{14} M_\odot} \right)^{1/4} \left( \frac{r_0}{100 \text{kpc}} \right)^{-3/4} \left( \frac{T}{\text{keV}} \right)^{-3/8} \quad (9)$$

where  $T$  is the X-ray temperature. The results are shown in Table 1. The minimum neutrino mass is  $2 - 3$  eV for these three clusters. Since the current limit is  $m_\nu < 2$  eV from tritium  $\beta$  decay<sup>6</sup>, our results in Table 1 are comparable to or larger than this limit.

Sanders (2003) derived a core radius of neutrino virialized halo,  $r_\nu \gtrsim 700 \text{kpc} (m_\nu/2\text{eV})^{-2} (T/\text{keV})^{-1/4}$ . But this is much larger than the core radius in Table 1. Hence, it is difficult to explain the small core in the neutrino halo model.

## 5. Conclusion

We have studied the weak lensing of galaxy clusters in MOND. We calculate the shears and magnifications of the background galaxies for three clusters (A1689, CL0024, CL1358) and 42 SDSS clusters, and compare them with the observational data. It turns out that the MOND cannot explain the data irrespective of  $g_0$  unless a dark matter halo is added. The above results are consistent with those of previous studies (e.g. Aguirre, et al. 2001; Sanders 2003). If the dark halo is composed of massive neutrinos, the mass of the neutrino should be heavier than  $2 - 3$  eV. Even with massive neutrinos, it is still difficult to form the small core (100–300 kpc) in the neutrino halo model.

We would like to thank Takashi Hamana for useful comments and discussions. TC was supported in part by a Grant-in-Aid for Scientific Research (No.17204018) from the Japan Society for the Promotion of Science and in part by Nihon University.

## REFERENCES

Aguirre, A., Schaye, J. & Quataert E. 2001, ApJ, 561, 550

Aguirre, A. 2003, in Proc. the IAU Symposium 220 "Dark Matter in Galaxies", ed. by S. Ryder, D.J. Pisano, M. Walker and K. Freeman, 17

Andersson, K.E. & Madejski, G.M. 2004, ApJ, 607, 190

Angus, G.W., Shan, H.Y., Zhao, H.S. & Famaey, B. 2006, astro-ph/0609125, submitted to ApJL

Arabadjis, J.S. Bautz, M.W. & Garmire, G.P. 2002, ApJ, 572, 66

Angus, G.W., Famaey, B. & Zhao, H.S. 2006, 371, 138

Bekenstein, J.D. 2004, Phys. Rev. D, 70, 083509

Broadhurst, T.J., Taylor, A.N. & Peacock J.A. 1995, ApJ, 438, 49

Broadhurst, T. et al. 2005, ApJ, 619, L143

Chiu, M.-C., Ko, C.-M. & Tian, Y. 2006, ApJ, 636, 565

Chen D.-M. & Zhao, H.S. 2006, ApJ, 650, L9

Clowe, D. et al. 2006, ApJ, 648, L109

Dye, S. et al. 2002, A&A, 386, 12

Gavazzi, R. 2002, New A Rev., 46, 783

Hoekstra, H., Franx, M., Kuijken, K., & Squires, G. 1998, ApJ, 504, 636

Kneib, J.P. et al. 2003, ApJ, 598, 804

Milgrom, M. 1983, ApJ, 270, 365

Mortlock, D.J. & Turner, E.L. 2001, MNRAS, 327, 552

Mortlock, D.J. & Turner, E.L. 2001, MNRAS, 327, 557

Pointecouteau, E. & Silk, J. 2005, MNRAS, 364, 654

Qin, B., Wu, X.P. & Zou, Z.L. 1995, A&A, 296, 264

Sanders, R.H. & McGaugh S.S. 2002, ARA&A, 40, 263

Sanders, R.H. 2003, MNRAS, 342, 901

Sheldon, E.S. et al. 2001, ApJ, 554, 881

Slosar, A., Melchiorri, A. & Silk, J.I. 2005, Phys. Rev. D, 72, 101301

<sup>6</sup>Particle Data Group Home Page : <http://pdg.lbl.gov/>

TABLE 1  
BEST FITTING MODEL FOR DARK HALO PROFILE AND NEUTRINO MASS.

	$M_0 (M_\odot)$	$r_0$ (kpc)	$T$ (keV)	$m_\nu$ (eV)
A1689	$(6.2 \pm 1.2) \times 10^{14}$	$125 \pm 52$	$9.00 \pm 0.13$	$> 3.6 \pm 1.1$
CL0024	$(3.5 \pm 1.0) \times 10^{14}$	$309 \pm 93$	$3.52 \pm 0.17$	$> 2.2 \pm 0.5$
CL1358	$(8.1 \pm 3.6) \times 10^{13}$	$134 \pm 68$	$7.16 \pm 0.10$	$> 2.2 \pm 0.9$

Skordis, C. 2005, submitted to Phys. Rev. D,  
astro-ph/0511591

Skordis, C., Mota, D.F., Ferreira, P.G., & Boehm  
C. 2006, Phys. Rev. Lett., 96, 011301

Tremaine, S. & Gunn, J.E. 1979, Phys. Rev. Lett.,  
42, 408

Zekser, K.C. et al. 2006, ApJ, 640, 639

Zhang, Y.-Y. et al. 2005, A&A, 429, 85

Zhao, H.S. et al. 2006, MNRAS, 368, 171

White, M. & Kochanek, C.S. 2001, ApJ, 560, 539

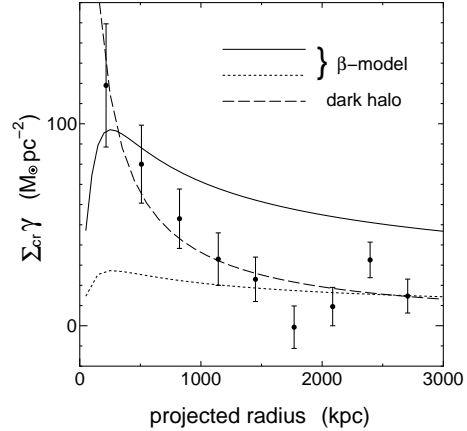


Fig. 5.— The mean shear of 42 SDSS clusters. The solid and dotted lines are the beta models, and the dashed line is the dark halo model.